

Phase I Topical Report

Project No. 42516

Date 06/2005 – 08/2006

#DE-FC26-05NT42516

Development of Sulfur and Carbon Tolerant Reforming Alloy Catalysts Aided by
Fundamental Atomistics Insights

PI: Suljo Linic

Suljo Linic

Assistant Professor

Department of Chemical Engineering

University of Michigan

Phone: 734-647-7984

Email: linic@umich.edu

Fax:

June/20/2006

Disclaimer	3
Abstract.....	4
Executive Summary	5
Executive Summary	5
2. Theoretical and Experimental Methods	8
2.1. Density Functional Theory (DFT) Methodology	8
2.2. Catalyst Synthesis	9
2.3. Reactor Setup	10
2.4. Catalyst Characterization: Microscopy and Spectroscopy	10
3. Results and Discussion.....	11
3.1 Experimental Studies of Carbon Poisoning.....	11
3.2 Quantum DFT Studies of Carbon/Ni interactions and Carbon Poisoning.....	13
3.3 Quantum DFT identification of novel carbon-resistant reforming alloy catalysts	15
3.3 Reactor testing and characterization of Sn/Ni alloy catalysts	18
4. Conclusions.....	21
5.1 Relevancy and future:.....	21
6.1 Special Recognitions & Awards/Patents Issued	23
6.2 Publications/Presentations	23
7. References	24

Disclaimer

This report was prepared as an account of work sponsored by an agency of the United States Government. Neither the US Government nor any agency thereof, nor any of their employees, makes any warranty, express or implied, or assumes any legal liability or responsibility for the accuracy, completeness, or usefulness of any information, apparatus, products, or process disclosed, or represents that its use would not infringe privately owned rights. Reference herein to any specific commercial product, process, or service by trade name, trademark, manufacturer, or otherwise does not necessarily constitute or imply its endorsement, recommendation, or favoring by the United States government or any agency thereof. The views and opinions of authors expressed herein do not necessarily state or reflect those of the United States Government of any agency thereof.

Abstract

Current hydrocarbon reforming catalysts suffer from rapid carbon and sulfur poisoning. Even though there is a tremendous incentive to develop more efficient catalysts, these materials are currently formulated using inefficient trial and error experimental approaches. We have utilized a novel hybrid experimental/theoretical approach, combining quantum Density Functional Theory (DFT) calculations and various state-of-the-art experimental tools, to formulate carbon tolerant reforming catalysts. We have employed DFT calculations to develop molecular insights into the elementary chemical transformations that lead to carbon poisoning of Ni catalysts. Based on the obtained molecular insights, we have identified, using DFT quantum calculation, Sn/Ni alloy as a potential carbon tolerant reforming catalyst. Sn/Ni alloy was synthesized and tested in steam reforming of methane, propane, and isooctane. We demonstrated that the alloy catalyst is carbon-tolerant under nearly stoichiometric steam-to-carbon ratios. Under these conditions, monometallic Ni is rapidly poisoned by sp² carbon deposits. The research approach is distinguished by a few characteristics: (a) Knowledge-based, bottom-up approach, compared to the traditional trial and error approach, allows for a more efficient and systematic discovery of improved catalysts. (b) The focus is on exploring alloy materials which have been largely unexplored as potential reforming catalysts.

Executive Summary

The envisioned shift to hydrogen economy driven by rapidly evolving fuel cell technology will require energetically feasible and environmentally friendly conversion of fossil, synthetic, and bio-renewable fuels into hydrogen. To realize this vision, major advances in catalysis are required. Improved hydrocarbon reforming, water gas shift (WGS), and preferential CO oxidation (PROX) catalysts need to be formulated and synthesized. These catalysts need to perform the desired reactions with utmost efficiencies, at reduced costs, and with improved durability. Even though there is a tremendous incentive to develop more efficient catalysts, these materials are currently formulated using inefficient trial and error experimental approaches. In this document we describe a novel hybrid experimental/theoretical effort aimed towards a bottom-up, knowledge-based formulation of carbon-tolerant reforming alloy catalysts.

Our objective is to utilize the hybrid experimental/theoretical framework to formulate and develop carbon- and/or sulfur-tolerant hydrocarbon reforming catalysts. Unlike current state-of-the-art catalysts, which are often monometallic metal particles (Ni is often used) adsorbed on oxide supports, we focus on oxide-supported metallic alloy catalysts. These catalysts would be utilized for hydrogen production from hydrocarbons and as robust anodes for direct electro-catalytic reforming over Solid Oxide Fuel Cells (SOFC).

In Phase I, we have employed quantum Density Functional Theory (DFT) calculations to develop molecular insights into the elementary chemical transformations that lead to carbon poisoning of Ni catalysts during steam reforming of hydrocarbons. The DFT calculations were utilized to calculate, from first principles, activation barriers and reaction energies for various elementary step chemical reactions. In the DFT studies, we demonstrated that:

1. Carbon atoms, formed in the process of hydrocarbon decomposition on Ni catalyst, either react with each other, forming sp² carbon networks, or with oxygen, forming CO which desorbs into the gas phase. Oxygen is formed on the catalysts surface in steam (water) splitting reactions.

2. The carbon tolerance of catalysts is governed by their capacity to selectively oxidize carbon atoms, while suppressing the formation of C-C bonds which yield extended sp²-carbon structures which deactivate the catalyst.
3. The main problem with monometallic Ni catalyst is that the rate of C-C bond formation is high, leading to the formation of carbon structures and to catalyst deactivation.
4. Guided by the insights outlined above (1-3), we have utilized DFT calculations to search for potential carbon-tolerant alloy catalysts. The main goal was to identify alloy catalysts that preferentially oxidize carbon atoms (promote C-O bond formation) and suppress the formation of extended carbon networks (suppress C-C bond formation). In our DFT calculations, we have identified Sn/Ni, Ag/Ni, and Au/Ni alloys as potential carbon-tolerant reforming catalysts.

The proposed mechanism of carbon poisoning that is dominated by carbon atom diffusion and C-C bond formation is in agreement with numerous characterization studies performed in our laboratories. These included scanning electron microscopy (SEM), transmission electron microscopy (TEM), energy dispersive x-ray spectroscopy (EDS), x-ray photoelectron spectroscopy (XPS), and x-ray diffraction (XRD).

The above describe results of DFT calculations, suggesting that Sn/Ni alloy should be more resistant to carbon poisoning than monometallic Ni, were tested in our reactor setup. We have synthesized Ni and Sn/Ni alloy catalysts supported on yttria-stabilized-zirconia (YSZ) and tested them in the steam reforming of methane, propane, and isooctane. In these studies we have mainly focused on catalysts with high metal loading (>30 % by weight) and large particle size (diameter of up to 1 μ m). Our reactor studies showed that Sn/Ni is much more stable than monometallic Ni. For example, while monometallic Ni catalyst deactivates within a few minutes in steam reforming of propane and isooctane at steam to carbon ratio of 1.5, the Sn/Ni catalyst is active and stable for as long as it was kept on stream. Furthermore, our electron- and photon-based characterization studies demonstrated that no traces of carbon were deposited on the alloy catalyst during its operation.

The main objectives of Phase II studies will be to:

- test the alloy catalysts that have not been tested in Phase I, mainly Ag/Ni and Au/Ni
- test the promising alloy materials (Sn/Ni, Au/Ni, Ag/Ni) in the reforming of heavier fuels such as C₁₀-C₁₅ alkanes (these are the main components of JP-8 and diesel). This is important since these fuels have longer carbon chains which are known to deactivate reforming catalyst more rapidly.
- test the alloy catalysts as potential Solid Oxide Fuel Cell (SOFC) anodes for direct electro-catalytic hydrocarbon reforming. The experiments will be performed in an SOFC test station, recently built in our laboratory.
- examine whether the performance of alloy catalysts could be improved by synthesizing smaller alloy particles. Our preliminary DFT calculations suggest that smaller catalytic particles should be more active and more carbon tolerant than the larger particles, that were analyzed in Phase I.
- utilize our theoretical tools to possibly further improve the catalyst composition.

The research approach outlined in the document is distinguished by a few characteristics: (a) Knowledge-based, bottom-up approach, compared to the traditional trial and error approach, allows for a more efficient and systematic discovery of improved catalysts. (b) The focus is on exploring alloy materials which have been largely unexplored as potential reforming catalysts. (c) Infrastructure at the University of Michigan is ideally suited for the proposed research plan. Recent additions of the Hydrogen Research Center and the Transportation Energy Center (TEC) will allow for an efficient execution of the proposed research plan.

Description of Phase I:

In Phase I we have employed hybrid experimental/theoretical approach – the approach combines quantum Density Functional Theory (DFT) calculations, catalyst synthesis, catalysts testing, and catalysts characterization – to identify potential carbon-tolerant reforming bimetallic catalysts. We are interested in the formulation of carbon-tolerant reforming catalysts since: (i) these catalysts are crucial for efficient H₂ production from renewable and fossil hydrocarbon fuels, (ii) the catalyst could be employed as anodes for direct internal hydrocarbon utilizations over Solid Oxide Fuel Cells (SOFC).

Below, we discuss the theoretical and experimental methodologies as well as the results of DFT quantum calculations, reactor testing, and catalyst characterization. This is followed by a conclusion section.

2. Theoretical and Experimental Methods

In this section we outline theoretical and experimental methodology. We first describe DFT quantum chemical calculations. This is followed by the description of catalyst synthesis methods and the reactor test-station. Lastly, we briefly describe various microscopic and spectroscopic tools that were employed to characterize the mechanism of carbon poisoning and also to characterize our alloy catalysts.

2.1. Density Functional Theory (DFT) Methodology

DFT is a methodology that is employed to efficiently solve quantum Schrodinger equation with high accuracy.^{1,2,3} For the development of DFT, Kohn and Sham received the Nobel prize in chemistry in 1998. Due to its accuracy and computational efficiency DFT has become, within the last ten years, the quantum computational tool of choice in solid state physics and surface chemistry.⁴ These tools have already had a significant impact on the discovery of efficient solid-state catalysts as corroborated by the DFT-driven discovery of novel ethylene epoxidation and ammonia synthesis catalysts.^{5,4}

DFT calculations allow us to obtain, from first principle and with high accuracy, the ground state geometries^{6,7,8} and energies^{6,7,8} of relevant reactants, products, and transition states involved in elementary chemical reactions on catalyst surfaces. For example, in Phase I DFT was utilized to investigate elementary chemical reactions of carbon atom metal surfaces. We have calculated the carbon atom diffusion and elementary surface reactions

over various reforming catalysts such as pure Ni and various alloys. This information can be obtained easily using DFT calculations while it is almost impossible to accurately acquire via other computational or experimental means. The DFT calculations were also utilized to identify promising carbon-tolerant alloy catalysts. We further elaborate on the DFT studies below in the document.

Along with DFT calculations we have employed various experimental tools to synthesize, test, and characterize the reforming catalysts.^{5, 9,10,6,7,8}

2.2. Catalyst Synthesis

As emphasized above, an important objective of our research was to assess the predictions of DFT calculations by synthesizing and testing the promising alloy catalysts, identified in our DFT studies.^{5,11} In order to synthesize these alloys we have utilized standard wet impregnation method and less conventional sequential ionic layer deposition (SILD) and atomic layer deposition (ALD). These synthesis methods allow for high control over the atomic structure and composition of catalysts.

Wet impregnation methods are based on liquid-phase impregnation of soluble salts on a support. Support is usually a metal oxide compound. Our steam reforming catalysts are supported on Ytria-Stabilized Zirconia (YSZ) The catalyst/support system is then calcined and reduced. We will elaborate on this synthesis technique further below when we the concrete results on Phase I studies.

SILD method is based on solution surface chemistry.^{12,13,14} Generally, SILD consists of successive treatments of a substrate surface with various solutions of salts, anions, and cations.^{12,13,14} Controlled surface reactions between these solution-stabilized ions and substrates yield well-defined materials. The advantage of this approach is that complex materials such as metal alloys can be synthesized with high control over their atomic structure and morphology.^{12,13}

Another synthesis technique that has been used recently to create various multi-component layered structures with atomic precision is ALD. ALD is based on standard chemical vapor deposition (CVD) technologies. In the ALD, a binary reaction is split into two half-reactions that occur on the surface of a substrate, i.e., the substrate actively participates in chemical reactions.^{15,16,17} Understanding of the relevant surface chemical reactions allows one to control precisely the structures of materials produced via ALD.

This technique has been used to create well-defined oxide layers on metal particles, and layers of one metal on other metals.¹⁵

2.3. Reactor Setup

The promising catalysts identified in our DFT calculations and synthesized using the above described methods were evaluated under steady state conditions in a reactor test-station using gas flows of N₂, fuel, and steam delivered through mass flow controllers.⁵ The reactor test-station consisted of a 20 mm I.D. quartz tube encased in a vertical tube furnace. We tested the catalyst in methane, propane, and iso-octane steam reforming. In the experiments we have systematically varied the concentration of steam and fuel. Analysis of the product gas stream was performed by in-line gas chromatography which utilizes thermal conductivity and flame ionization detectors.

2.4. Catalyst Characterization: Microscopy and Spectroscopy

As stated above we have also characterized fresh and used catalysts with various characterization techniques. We have employed transmission electron microscopy (TEM), scanning electron microscopy (SEM), energy dispersive x-ray spectroscopy (EDS), x-ray photoelectron spectroscopy (XPS), and x-ray diffraction (XRD). These techniques allowed us to determine the morphology and atomic composition of the catalytic particles as well as the nature of carbon deposits that deactivate the catalysts. Below we describe the equipment and the information that can be acquired with these tools.

Jeol 2010F electron microscope was used for EDS, STEM, and TEM studies. The instrument operates under vacuum conditions of 1.5×10^{-7} torr. The instrument utilizes a zirconated tungsten (100) thermal field emission tip filament. The EDS measurements were obtained via Ametec EDAX system in spot and scanning modes. The lens conditions were set for a probe size of 0.5 nm to obtain adequate probe current. To minimize the effect of specimen drift, a drift correction mode was used during elemental mapping. For each sample we have analyzed several particles from several different areas.

SEM is an electron-based microscopy that is utilized to investigate the morphology and size of catalytic particles that are larger than ~50 nm. SEM detects secondary electrons that are created after primary electrons interact with a sample surface. SEM is employed to image fairly large (compared to TEM) areas of a sample. TEM is a

transmission electron-based microscopy that is employed to image catalytic particles with atomic resolution. TEM is based on the detection of the primary electrons that are transmitted through the sample. TEM and SEM are usually used in tandem with the energy dispersive x-ray spectroscopy (EDS), which analyzes the x-rays that are emitted in the process of the electron-sample collisions. The emitted x-rays provide the element-specific fingerprint of catalytic particles. Coupling EDS with scanning mode TEM allows one to obtain the atomic information about the arrangement of different atoms in catalytic particles. These atom-specific insights are particularly useful when working with alloys where the information about the mixing of the alloy constitutive elements is crucial.

We have also utilized XPS, a photon-based spectroscopy, to analyze the electronic structure and the elemental composition of our catalysts. The advantage of XPS is that it is a surface sensitive technique. We have employed Kratos Axis Ultra XPS with 150 W Al (Mono) X-ray gun. This instrument was operated ex-situ under pressure of 5×10^{-9} torr. The analyzed samples were left under vacuum over night before taking data. The runs were conducted using pass energy of 40 eV. The charge neutralizer was utilized to prevent sample charging. The instrument was calibrated with respect to Au 4f_{7/2} at 84 eV.

The X-ray diffraction (XRD) measurements were conducted with a Cu-K α source using a Philips XRG5000 3 kW x-ray generator with crystal alignment stage and Rigaku thin film camera. The spectrum was analyzed using Jade v.7 software. XRD was employed to obtain the structural information about the catalysts and carbon deposits that are formed during the reforming process.

3. Results and Discussion

3.1 Experimental Studies of Carbon Poisoning

Critical issue in hydrocarbon reforming is that current reforming catalysts such as Ni facilitate the formation of carbon structures which deactivate the catalyst.^{18,19,20,21,22,23} The formation of carbon deposits can be partially suppressed by an introduction of steam (steam reforming) which oxidizes and removes the deposited carbon atoms therefore preserving the catalyst surface.²⁴ Steam reforming is an endothermic process which requires high operating temperatures.

Steam reforming: $C_nH_m + n H_2O \rightarrow (n+m/2) H_2 + n CO$

Metallic Ni is often used as the catalyst for steam reforming and generally very high concentrations of steam are required to prevent carbon poisoning of Ni. However, high steam concentration is not desirable since it lowers the energy density of the products. For example, when H_2 is produced by direct steam reforming in SOFCs, the low density of H_2 leads to low SOFC current density and low power output.^{25,26} It is imperative to design carbon-tolerant reforming catalysts that can operate with low steam concentrations.^{27,28} Optimal catalysts would utilize one H_2O molecule per one carbon atom in a hydrocarbon, i.e., these catalysts would operate at the steam-to-carbon ratio of one. Current reforming catalysts such as Ni are rapidly poisoned by carbon deposits at this steam to carbon ratio.

To illustrate the problem of carbon poisoning, in Figure 1 we show the results of our experimental studies where the deactivation of Ni catalyst supported on YSZ during CH_4 steam reforming was investigated.

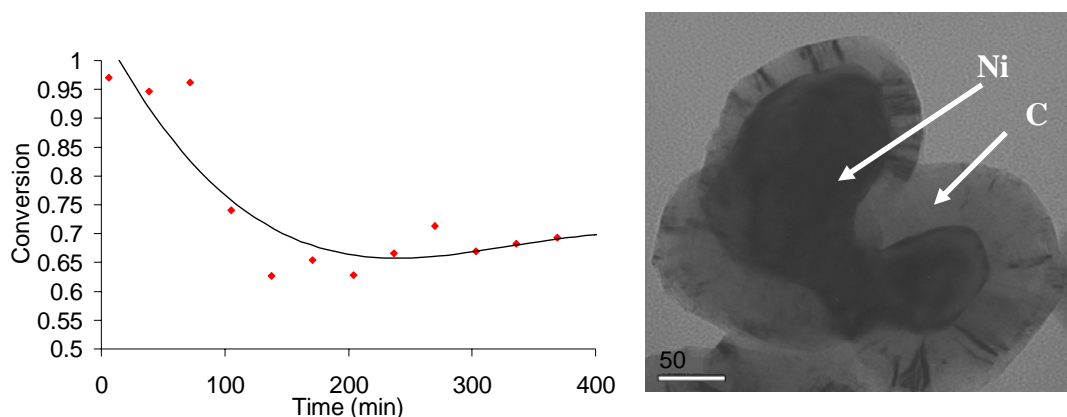


Figure 1: (a) Methane conversion over Ni/YSZ (Ni supported on YSZ) catalyst as a function of the time on stream. Steam to carbon ration was 0.5. (b) TEM studies show that thick graphitic carbon deposits are formed on the Ni catalyst during methane reforming process.

It is observed that the catalyst activity decreases as a function of the time on stream. The deactivation is a consequence of the formation of large deposits of sp²-carbon networks. TEM, EDS, and XRD experiments were also utilized to detect the graphitic carbon on Ni catalyst. We note that we have observed even more dramatic poisoning of Ni catalysts for heavier hydrocarbon fuels.

We have investigated, using quantum DFT calculations, the underlying molecular processes that lead to carbon poisoning. The goal of these DFT studies was to develop molecular insights into the mechanisms that govern the catalyst poisoning and to formulate a rational approach towards the design of carbon-tolerant steam reforming catalysts. The results of these calculations are outlined in the next sections.

3.2 Quantum DFT Studies of Carbon/Ni interactions and Carbon Poisoning

We have utilized DFT calculations to calculate, from first principles, the elementary step reaction energies associated for methane steam reforming on Ni(111), see Figure 2. It is important to note that DFT allows us to obtain the reaction energies accurately and efficiently. This information is difficult to acquire via other means.

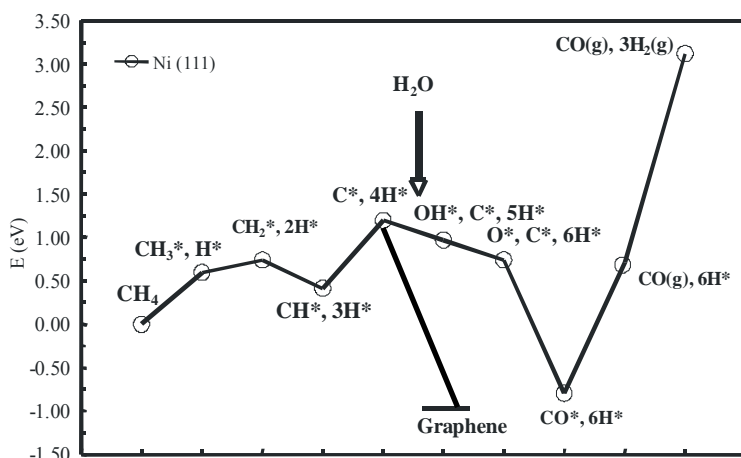
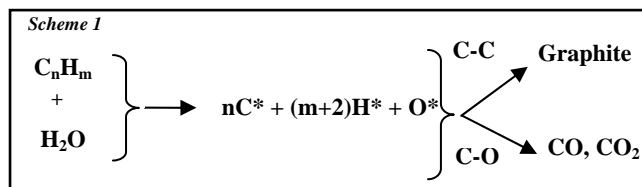


Figure 2: DFT-calculated reaction coordinate for steam reforming of methane over Ni(111). The figure demonstrates that the thermodynamically stable state of carbon is graphene. To prevent the catalyst poisoning, the formation of the graphitic sheets needs to be prevented

The DFT-calculated reaction coordinate clearly demonstrates that thermodynamically the most stable state of carbon on Ni(111) is a graphene sheet adsorbed on the surface. For example, we calculate that the adsorption energy for a carbon atom in a graphite sheet on Ni(111) is by ~2 eV more exothermic than the adsorption energy for individual carbon atoms adsorbed on Ni(111) at $\frac{1}{4}$ ML coverage. Clearly, there is a strong thermodynamic driving force for carbon atoms to form deposits of sp²-carbon. The tendency to form sp² carbon structures is the main reason for the rapid deactivation of Ni catalysts.

Furthermore, Figure 2 also demonstrates that carbon atoms, created in the process of hydrocarbon decomposition on Ni, can be removed from the surface by their oxidation and the formation of CO. Oxygen that oxidizes carbon atoms is formed by the splitting of water (steam) on Ni. The DFT studies suggest that the long term stability of reforming catalysts is governed by their ability to selectively oxidize carbon (form C-O bonds) and remove it from the surface, while preventing the formation of C-C bonds as shown in Scheme 1.



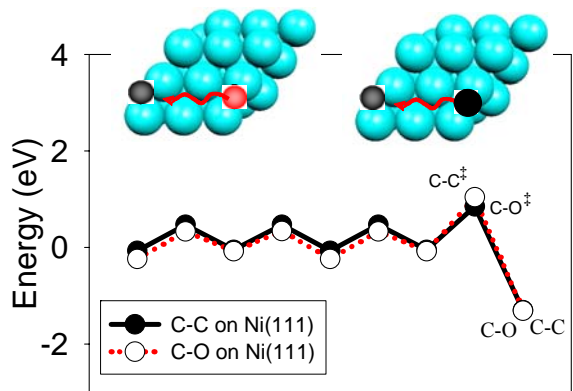
Scheme 1: Carbon atoms can either react with each other to form sp²-carbon deposits which deactivate the catalyst, or they are oxidized to form CO which desorbs from the surface.

Motivated by these insights, we have further utilized DFT to investigate the elementary steps associated with C-C and C-O bond formation on Ni. In order for C-C bonds to form on a catalyst surface, C atoms need to diffuse on the surface and collide with each other²⁹. Similarly, oxidation of carbon atoms requires collisions between C and O atoms on the surface. We have employed DFT to calculate activation barriers for C and O atoms diffusion and the activation barriers for C-O and C-C bond formation.

Figure 3 (dark line) depicts the potential energy surface associated with C atom diffusion and subsequent C-C bond formation on Ni(111). We observe that the activation barrier for C atom diffusion on Ni(111) is ~ 0.5 eV (50 kJ/mol), suggesting that C atoms are very mobile on the surface. We also calculate that the activation barrier for the formation of C-C bonds is fairly low ~0.92 eV. The high rate of C atom diffusion and the low activation barrier for C-C bond formation result in the rapid formation of extended sp²-carbon deposits, ultimately leading to Ni deactivation.^{23,24,30}

Figure 3 also depicts the potential energy surface for C-O bond formation on Ni(111) (dotted red line). The Figure demonstrates that on Ni(111) the chemical pathways leading to C atom oxidation (C-O bond formation) have comparable overall activation barriers as those for the C-C bond formation. Similar activation barriers associated with the C-O and C-C bond formation on Ni suggest that this is not an ideal reforming catalyst. Simply stated, the rate of C-C bond formation is too high to ensure the long lifetime of Ni catalysts.

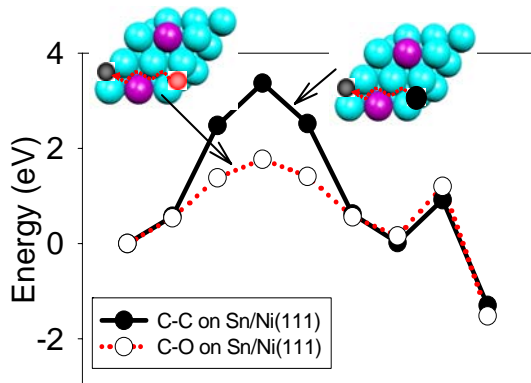
Figure 3: DFT calculated energies for C and O atom diffusion and C-O and C-C bond formation on Ni(111). Full dark lines represent the energy landscape associated with the C-C bond formation, while red dotted lines represent the energy for C-O bond formation. $C-C^\ddagger$ represents the DFT calculated energy for the transition state for C-C bond formation, while $C-O^\ddagger$ depicts the transition state for C-O bond formation. Inserts show the lowest energy pathways for C-C (right panel) and C-O (left panel) bond formation on Ni(111) surface. The pathways consists of C (dark atom, right panel) or O (red atom, left panel) atom diffusion over the surfaces and subsequent formation of C-C and C-O bonds respectively.



3.3 Quantum DFT identification of novel carbon-resistant reforming alloy catalysts

We have further utilized DFT calculations to investigate C-O and C-C bond formation on various Ni-containing alloys. The objective of these studies was to identify alloy catalysts that might be more carbon-tolerant than monometallic Ni. Optimal catalysts will, relative to monometallic Ni, favor carbon oxidation (C-O bond formation) over C-C bond formation. In our DFT calculations we have determined that Au/Ni, Ag/Ni and Sn/Ni alloy catalysts are good candidates for carbon-tolerant reforming. The alloy material that emerged as the most promising in the DFT studies was Sn/Ni. The results of the DFT calculations for Sn/Ni are shown in Figure 4.

Figure 4: DFT calculated energies for C and O atom diffusion followed by the respective C-C and C-O bond formation on Sn/Ni(111). Full dark lines represent the energy landscape associated with the C-C bond formation, while red dotted lines represent the energy for C-O bond formation. Inserts show the lowest energy pathways for C-C (right panel) and C-O (left panel) bond formation on Sn/Ni(111) surface. The pathways consists of C (dark atom, right panel) or O (red atom, left panel) atom diffusion over the surfaces and subsequent formation of C-C and C-O bonds respectively. Notice that the activation barrier for C-C bond formation is much larger than the one for C-O bond formation. Sn atoms are large red spheres, Ni atoms are large light blue spheres.



The DFT calculations presented in Figure 4 show that on Sn/Ni surface alloy – surface alloy is characterized by Sn displacing Ni atoms from the top Ni(111) layer – the

relative kinetics of C-O and C-C bond formation is significantly different than on Ni. For example the kinetic barriers for C (full dark lines) and O (dotted red lines) atom diffusion on Sn/Ni(111) surface are by 1.9 and 1.2 eV larger than the respective kinetic barriers on Ni(111). The dramatic Sn-induced increase in the diffusion barriers suggests that over Sn/Ni, C and O atom diffusion becomes kinetically-limiting for the respective C-C and C-O bond formation. The DFT calculations suggest that on the alloy surface the rate of C-oxidation is much greater than the rate of C-C bond formation. We note that on Ni(111), the rates of C-O and C-C bond formation were similar to each other, see Figure 3. The DFT studies imply that the growth of carbon deposits should be suppressed by alloying Sn into the Ni lattice since carbon atoms will preferentially react with oxygen forming CO rather than react with other carbon atoms.

Furthermore, our DFT calculations show that the formation energy of Sn/Ni surface alloy is lower than the formation energy of Sn bulk alloys or the formation energy corresponding to separate, pure Sn and Ni phases. We calculate an alloy formation energy as:

$$E = E(\text{Ni/Sn_slab}) - E(\text{Ni_slab}) - \mu(\text{Sn}) + \mu(\text{Ni})$$

where $E(\text{Ni/Sn_slab})$ is the DFT calculated energy of a 3x3x4 alloy slab with an Sn atom displacing a Ni atom either in surface of bulk, $E(\text{Ni_slab})$ is the DFT calculated energy of 3x3x4 Ni slab, while $\mu(\text{Sn})$ and $\mu(\text{Ni})$ are chemical potentials of Sn and Ni atoms respectively. $\mu(\text{Sn})$ and $\mu(\text{Ni})$ were obtained in DFT calculations as energies per atom associated with bulk Sn and bulk Ni respectively. The bulk calculations were performed for fcc Ni and cubic Sn lattice.

The above formulation of the formation energy sets up a pure Ni_slab as the reference state with the formation energy of zero. The formation energy associated with Sn/Ni surface alloy (one Sn atom replaces one Ni atom in the Ni top layer) was -2.044 eV/A², while the bulk alloy (one Sn atom in the second layer) has the positive energy of 1.67 eV/A². We note that we report the formation energy in the units of energy per unit area, i.e., the energy has been normalized to the area of the unit cell. Since we utilize 3x3x4 unit cell in all calculation, this does not have any impact on our conclusions.

The observation that Sn/Ni surface alloy has lower formation energy than the bulk alloy or the configuration corresponding to separate Sn and Ni phases is important since it suggests that there is a strong thermodynamic driving force to form and sustain Sn/Ni surface alloy. We have also calculated that aside from the formation of Sn/Ni surface alloy, there is a favorable thermodynamic driving force for Sn to displace Ni atoms from the step-edge sites or to decorate the step-edge sites on Ni substrate. In these configurations the Sn atoms, adsorbed in or on the edge sites, effectively repel C atoms from the low-coordinated step sites. Since low-coordinated step sites have been proposed to play an important role in the nucleation and growth of carbon deposits over Ni, this arrangement of Sn atoms would further lower the propensity of the alloys to form carbon deposits.

According to the above presented DFT calculations a small amount of Sn alloyed into a Ni catalyst surface should improve the stability of the catalyst by increasing the activation barrier for C-C bond formation and therefore preventing the formation of the deposits of sp²-carbon.

To summarize, the main conclusions of our DFT calculations are:

1. Carbon atoms, formed in the process of hydrocarbon decomposition on a reforming catalyst, react either with other carbon atoms, forming sp² carbon networks, or with oxygen, forming CO which desorbs into the gas phase.
2. The main problem with monometallic Ni catalyst is that the rate of C-C bond formation is high, yielding extended sp²-carbon structures, which deactivate the catalyst.
3. Carbon-tolerant reforming catalysts should preferentially oxidize carbon atoms (promote C-O bond formation) and suppress the formation of extended carbon networks (suppress C-C bond formation).
4. We have identified Sn/Ni alloy as potential carbon-tolerant reforming catalyst. The main advantage of Sn/Ni with respect to monometallic Ni is that the activation barrier for C-O bond formation is much lower than the barrier for C-C bond formation. We note that on pure Ni, the activation barriers for C-O and C-C bond formation are comparable.

The predictions of these calculations were examined in our experimental studies where pure Ni and Sn/Ni alloy catalysts were tested in a reactor setup in the steam reforming of methane, propane, and isooctane. So far, we have only tested Sn/Ni alloy and we plan to test Au/Ni and Ag/Ni in near future.

3.3 Reactor testing and characterization of Sn/Ni alloy catalysts

Pure Ni catalysts were prepared using the wet impregnation technique, with Ni nitrate salt and ethanol as the solvent. The catalytic particles were supported on yttria-stabilized-zirconia (YSZ). The dried precursor was thermally reduced at 600 °C in a calcination furnace for approximately 4 hours. The Ni weight loading for these catalysts was approximately 25%. We use YSZ support and the high weight loading of Ni since these catalysts could possibly be utilized as SOFC anodes where ion-conducting supports and high metal loading are required to achieve acceptable electron and ion conductivity. For Sn/Ni alloy catalysts, Sn was added (1-5% by weight with respect to Ni loading) in the aqueous form as a Sn-chloride salt, to the reduced Ni catalyst via wet impregnation. Following the addition of the Sn salt, the catalyst was dried for 12 hours at 100 °C and then reduced at 900 °C for 2 hr.

All catalysts were evaluated at steady state conditions in a flow reactor using gas flows of a hydrocarbon, H₂O, and N₂ delivered through mass flow controllers. The reactor consisted of a 20 mm I.D. quartz tube encased in a vertical tube furnace. Analysis of the product gas stream was performed by in-line gas chromatography. The gas chromatograph utilized thermal conductivity and flame ionization detectors to give quantitative analysis of all gaseous products.

The results of steam reforming of methane and isooctane over Ni and Sn/Ni catalyst are shown Figure 5. Sn/Ni alloy catalyst contained 1% Sn by weight with respect to Ni loading. The methane reforming experiments were performed with steam-to-methane ratio of 0.5, while isooctane reforming was performed at steam-to-carbon ratio of 1.5. Figure 5 illustrates that Sn/Ni is much more stable than monometallic Ni. For example, we observe that in isooctane steam reforming monometallic Ni catalyst deactivates within a few minutes. Similar results were obtained in the reforming of propane. The deactivation is accompanied by a large pressure drop across the reactor which is a consequence of a rapid buildup of carbon deposits.

Post isooctane reforming X-ray Photoelectron Spectroscopy (XPS) for monometallic Ni catalyst, shown in Figure 5b, demonstrates that the catalyst is completely covered by carbon deposits. While Ni electronic signal was not detected, we observed C 1s signals at 284.5 eV, indicative of sp² carbon, and 283.1 eV, which we assign to C atoms in intimate contact with the metal. In post-reaction XPS analysis of Sn/Ni, Ni 2p_{3/2} signal was detected at 253 eV corresponding to metallic Ni, while C electronic fingerprint was not measured. These results are consistent with the thesis that carbon deposits did not accumulate on the Sn/Ni catalyst.

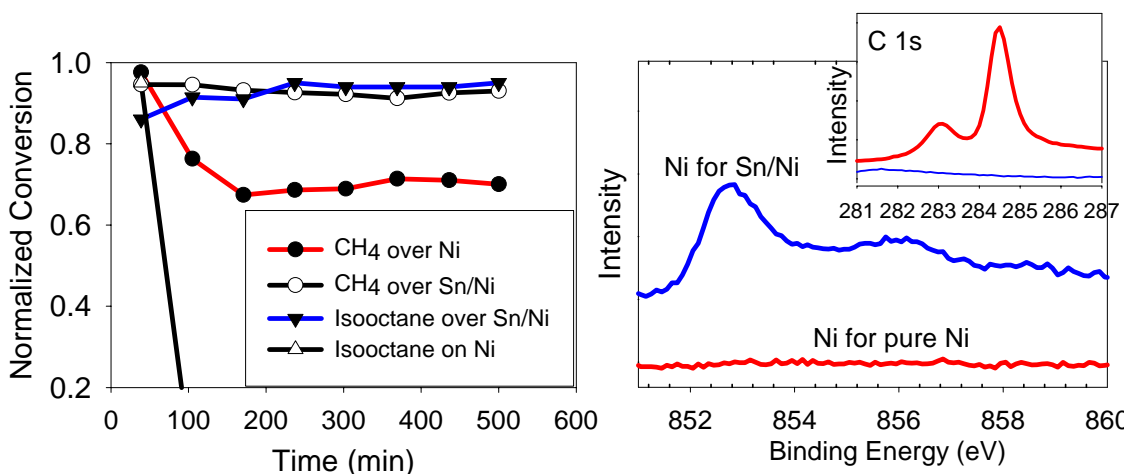


Figure 5: (a) H₂ yield obtained in steam reforming of isooctane over Sn/Ni alloy catalyst supported on YSZ at the steam-to-carbon ratio of 1.5. Pure Ni supported on YSZ rapidly deactivates under these conditions, while Sn/Ni is very stable. (b) XPS spectra in the energy range corresponding to Ni signal. Ni signal is very strong for the used Sn/Ni alloy supported on YSZ catalyst. On the other hand, Ni signal could not be detected for monometallic Ni supported on YSZ catalyst. The reason for this was that Ni catalyst is covered by carbon deposits as is illustrated in the insert where the XPS spectrum corresponding to carbon peak was collected for pure Ni catalyst. The carbon XPS spectrum suggests that Ni catalyst is completely covered with carbon deposits.

As suggested above the main reason for the exhibited robustness of Sn/Ni alloy catalyst is its resistance to the formation of extended carbon structures, as had been predicted in our DFT calculations. This is further corroborated by the XRD (x-ray diffraction) studies, shown in Figure 6(a) and STEM imaging shown in Figure 6(b). The XRD experiments showed that YSZ-supported Ni catalyst yields graphitic carbon in the reforming of all tested fuels, while Sn/Ni catalyst supported on YSZ does not produce any graphitic carbon structures, see Figure 6.

Figure 6(b) shows post-reaction STEM images of Ni and Sn/Ni catalysts. Elemental analysis (EDS) coupled with the STEM studies confirmed that Sn/Ni alloy catalyst did not form carbon deposits on catalyst surface while pure Ni catalyst is completely poisoned with carbon deposits.

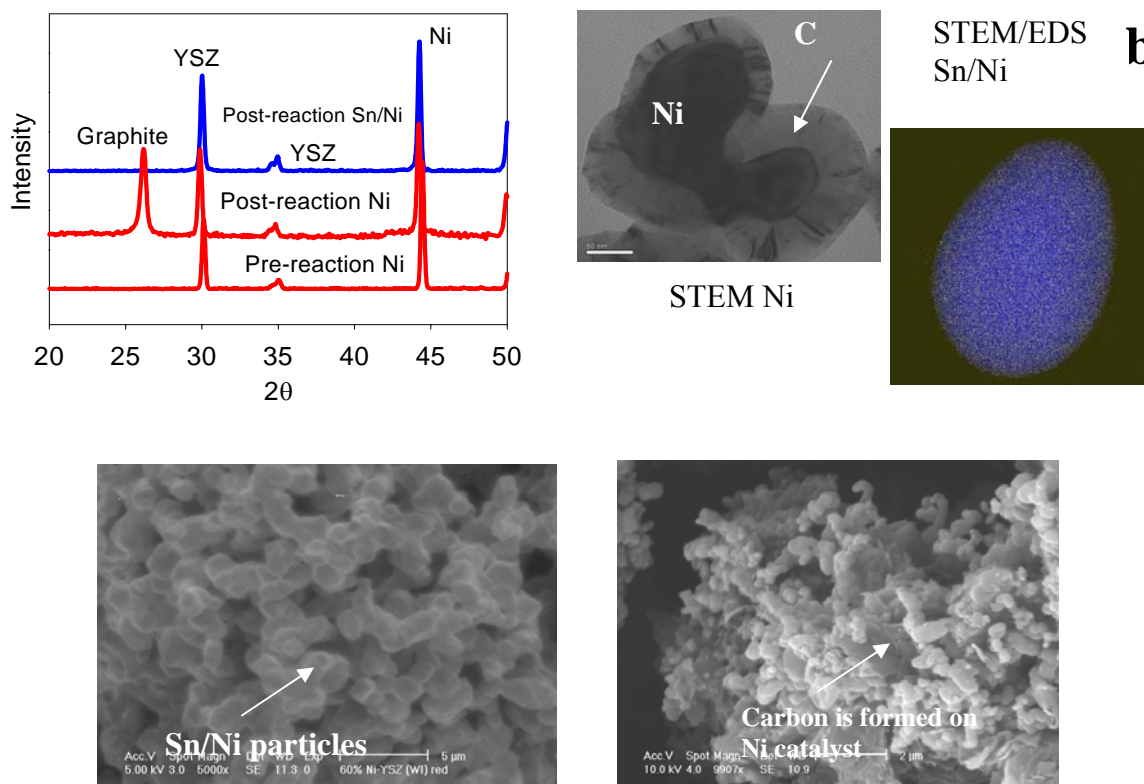


Figure 6. (a) XRD results for catalyst before and after isooctane reforming. XRD spectra for post- and pre-reaction Ni catalyst and post-reaction Sn/Ni catalyst are shown. Graphite peak is observed over Ni catalyst. (b) Post-isooctane reforming STEM spectra of Ni and Sn/Ni. Ni particles are completely covered with carbon deposits while Sn/Ni is carbon-free. Furthermore, elemental mapping of Sn/Ni particles via EDS suggests Sn surface alloying. Sn pixels are colored yellow, while Ni is blue. (c) SEM micrographs of Sn/Ni catalyst and Ni catalyst after isooctane steam reforming. Ni is completely covered by carbon deposits.

The studies presented above demonstrate that Sn/Ni alloy formulated in the first principles DFT calculations is a very promising carbon-tolerant steam reforming catalyst that is robust under fairly low steam-to-carbon ratios. This catalyst is far superior to monometallic Ni catalyst which rapidly deactivates during hydrocarbon reforming.

We also note that our preliminary DFT studies suggested that Ni/Au and Ni/Ag alloys hold promise as carbon-tolerant reforming catalysts. However, to date we have not investigated these alloys under steady-state reforming conditions.

4. Conclusions

We have utilized DFT quantum calculations to develop molecular insights into the mechanism of carbon poisoning. The results of the DFT calculations were supported by various microscopic (TEM, EDX, SEM, XRD), and spectroscopic (XPS, EDS) studies. We have identified carbon-atom diffusion and carbon-carbon bond formation as two critical elementary processes that lead to the formation of extended sp²-carbon networks which deactivate Ni catalysts. We have also determined that the long-term stability of steam reforming catalysts is governed by their capacity to selectively oxidize carbon atoms while suppressing C-C bond formation.

DFT calculations were further utilized to identify from first principles alloy materials which, as compared to monometallic Ni, have lower activation barrier for C-O bond formation and higher activation barriers for C-C bond formation. These DFT studies showed that Sn/Ni is more efficient in oxidizing and removing carbon atoms than Ni. The predictions of DFT calculations were tested in a reactor test station.

We have synthesizing YSZ-supported Sn/Ni and Ni catalysts using wet impregnations methods, and tested these catalysts in steam reforming of methane, propane, and isooctane. The steam-to-carbon ratio in these experiments ranged from 0.5 for methane to 1.5 for isooctane and propane. The reactor studies conclusively demonstrated that Sn/Ni catalyst is much more robust than monometallic Ni for all fuels. For example, we find that Ni catalyst is rapidly poisoned by carbon deposits in the steam reforming of propane and isooctane within a few minutes. On the other hand, Sn/Ni alloy is stable for as long as it was kept on stream. Our experimental characterization studies combining SEM, TEM, EDX, XPS, and XRD supported the predictions of DFT calculations and demonstrated that the main reason for the robustness of the alloy catalyst is that its resistance to the formation of sp² carbon networks.

5.1 Relevancy and future:

The work outlined above is distinguished by a few characteristics:

- (a) It represents a rare example where molecular level information was utilized directly to formulate an improved solid state catalyst. This is very important for further development of the field and it suggests that similar knowledge-based, as opposed to trial and error, approaches could be employed to address many issues related to hydrogen economy. Particularly intriguing is the research approach that combines state-of-the-art experiments and theory towards formulating more efficient solid state catalysts. It is our belief that alloy materials provides exciting opportunity for novel, active, selective, and stable catalysts.
- (b) In our studies we have focused on catalysts with high metal loading (>25 % by weight) supported on YSZ. High metal loading assures that these materials will conduct electrons, while YSZ was used since it is a high-temperature O^{2-} ion conductor. We decided to focus on these materials since they could be employed as Solid Oxide Fuel Cell (SOFC) anodes for direct, internal hydrocarbon reforming. The potential application of these materials as SOFC anodes will be explored in Phase II where we will test Sn/Ni alloys as SOFC anodes in our fuel cell testing station. The performance of Sn/Ni/YSZ SOFC anode catalyst will be compared to the performance of other materials that are utilized in direct hydrocarbon reforming such as Cu/CeO₂ and those that require indirect reforming such as Ru/CeO₂/YSZ in contact with Ni/YSZ.
- (c) The formulation of the carbon-tolerant catalysts for the reforming of fossil and bio-renewable hydrocarbons is imperative for the feasible hydrogen economy. While we have mainly focused, since we were interesting in possible SOFC applications, on Sn/Ni catalyst at the limit of high catalyst loading and fairly large catalytic particles (up to 1 micron), we also need to explore the reforming activity of these materials in the limit of lower loading and smaller particle size. Preliminary DFT studies indicate that the step and edge sites on our alloy catalyst should be more active for C-H bond activation. This implies that the catalytic particles with high concentration of step and edge sites should have an enhanced catalytic activity. One way to increase the concentration of step and edge sites on a catalytic particle is to synthesize smaller particles. For example, it is known that

catalytic particles in nano-meter range have an increased concentration of step sites. This will be another focus of Phase II.

6.1 Special Recognitions & Awards/Patents Issued

1. Nikolla, E. Schwank, J. Linic, S: Best Paper Presentations, “Experimental/Theoretical Studies Aimed at the Development of Carbon-Tolerant Catalysts”, Michigan Catalysis Society Annual Meeting 2006, Dow Chemicals, Midland, MI, May 2006
2. Nikolla, E. Schwank, J. Linic, S: Best Paper, “Controlling Carbon Chemistry via alloying: Hybrid Experimental/theoretical Approach”, University of Michigan Engineering Competition 2006, Ann Arbor, MI, March 2006

6.2 Publications/Presentations

1. Nikolla, E. Holowinski, A. Schwank, J. Linic, S., “Controlling Carbon Surface Chemistry by Alloying: Carbon Tolerant Reforming Catalyst”, Journal of the American Chemical Society, submitted 2006
2. Nikolla, E. Schwank, J. Linic, S., “Carbon Tolerant Alloy Catalyst for H₂ Production”, Journal of Catalysis, submitted 2006
3. Nikolla, E. Linic, S., “Hybrid Experimental/Theoretical Approach Aimed at the Development of Carbon Tolerant Alloy Catalyst”, ACS Colloids and Surface Science Meeting 2006, Bolder, Colorado, Jun 2006
4. Nikolla, E. Linic, S., “Hybrid Experimental/Theoretical Approach Aimed at the Development of Carbon Tolerant Alloy Catalyst”, NETL Contactors Meeting 2006, Pittsburg, Pennsylvania, Feb 2006
5. Nikolla, E. Schwank, J. Linic, S, “Experimental/Theoretical Studies Aimed at the Development of Carbon-Tolerant Catalysts”, Michigan Catalysis Society Annual Meeting 2006, Dow Chemicals, Midland, MI, May 2006

7. References

- ¹ DACAPO online user's manual:
<http://www.fysik.dtu.dk/CAMPOS/Documentation/Dacapo/OverView.html>, 2003.
- ² te Velde, G., F.M. Bickelhaupt, E.J. Baerends, C. Fonseca Guerra, S.J.A. van Gisbergen, J.G. Snijders, and T. Ziegler, "Chemistry with ADF". *Journal of Computational Chemistry*, 2001. **22**: p. 931-967.
- ³ Kootstra, F., *Time-dependent density functional theory for periodic systems*. 2001, Ph.D. Thesis, Rijksuniversiteit: Groningen, the Netherlands. p. 1-167.
- ⁴ B. Hammer, J.K. Nørskov, "Theory of adsorption and surface reactions" in (eds.) R. Lambert and G. Pacchioni, NATO ASI Series E, Kluwer Academic Publishers, Dordrecht 1997
- ⁵ S. Linic, J. Jankowiak, M.A. Barteau, "Selectivity driven design of bimetallic ethylene epoxidation catalysts from first principles", **Journal of Catalysis** (Priority Communication), **2004**, 224, 489.
- ⁶ S. Linic, M. A. Barteau, "Formation of a Stable Surface Oxametallacycle that Produces Ethylene Oxide", *Journal of American Chemical Society*, 2002, **124**: 310-317.
- ⁷ S. Linic, M. A. Barteau, "Construction of a Reaction Coordinate and a Microkinetic Model for Ethylene Epoxidation on Silver from DFT Calculations and Surface Science Experiments", *Journal of Catalysis*, 2003, **214**: 200-212.
- ⁸ S. Linic, J.W. Medlin, M.A. Barteau "Synthesis of Oxametallacycles from 2-iodoethanol on Ag(111) and the Structure Dependence of their Reactivity", *Langmuir*, 2002, **18**: pg 5197-5204.
- ⁹ S. Linic, M. A. Barteau, "Control of Ethylene Epoxidation Selectivity by Surface Oxametallacycle", *Journal of the American Chemical Society*, 2003, **125**, 4034.
- ¹⁰ S. Linic, M.A. Barteau, "On the Mechanism of Cs promotion in Ethylene Epoxidation on Ag", *Journal of the American Chemical Society*, 2004, **126**, 8086.
- ¹¹ Jacobsen, C.J.H., S. Dahl, A. Boisen, B.S. Clausen, H. Topsøe, A. Logadottir, and J.K. Nørskov, "Optimal catalyst curves: Connecting density functional theory calculations with industrial reactor design and catalyst selection". *Journal of Catalysis*, 2002. **205**: p. 382-387.
- ¹² L.B. Gulina, V.P. Tolstoy, "Synthesis of Ag₇SbS₇ nanolayers on the silica by ionic layer deposition, **Russian Journal of General Chemistry**, 2002, 72(6): 899-903.
- ¹³ G. Korotcenkov, V. Macsanov, V. Brinzari, V. Tolstoy, J. Schwank,

A. Cornet, J. Morante, "Influence of Cu-, Fe-, Co-, and Mn-oxide nanoclusters on sensing behavior of SnO₂ films", **Thin Solid Films**, 2004, **457**: 209-214

¹⁴ V.P. Tolstoy, *Thin Solid Films* 307 (1997) 10.

¹⁵ Jeffrey R. Wank, Steven M. George, Alan W. Weimer, "Coating Fine Nickel Particles with Al₂O₃ Utilizing an Atomic Layer Deposition-Fluidized Bed Reactor (ALD-FBR)", **Journal of American Ceramic Society**, 2004, 87: 762-765.

¹⁶ S. M. George, A. W. Ott, and J. W. Klaus, "Surface Chemistry for Atomic Layer Growth," **Journal of Physical. Chemistry**, 1996, 100: 13121-13131.

¹⁷ S. M. George, A. W. Ott, and J. W. Klaus, "Atomic Layer Growth Using Binary Reaction Sequence Chemistry"; p. 41-PHYS in **Abstracts of Papers of the American Chemical Society**, 213. American Chemical Society, Columbus, OH, 1997.

¹⁸ SECA Workshop Proceedings (I-IV) and Core Technology Workshop Proceedings, www.seca.doe.gov

¹⁹ Proceedings of the European Solid Oxide Fuel Cell Forum (I-VI), Lucerne, Switzerland, www.efcf.com

²⁰ Triantafyllopoulos, N.C. and S.G. Neophytides, *The nature and binding strength of carbon adspecies formed during the equilibrium dissociative adsorption of CH₄ on Ni-YSZ cermet catalysts*. *Journal of Catalysis*, 2003. **217**(2): p. 324-333.

²¹ McIntosh, S., et al., *An examination of carbonaceous deposits in direct-utilization SOFC anodes*. *Journal of the Electrochemical Society*, 2004. **151**(4): p. A604-A608.

²² Vernoux, P., J. Guindet, and M. Kleitz, *Gradual internal methane reforming in intermediate-temperature solid-oxide fuel cells*. *Journal of the Electrochemical Society*, 1998. **145**(10): p. 3487-3492

²³ Besenbacher, F, Chorkendorff, I, Clausen, B.S., Hammer, B, Molenbroek, A.M., Norskov, J.K., Stensgaard I., "Design of a surface alloy catalyst for steam reforming", *Science*, 1998, 279: p. 1913-1915.

²⁴ H. S. Bengaard, J. K. Nørskov, J. Sehested B. S. Clausen L. P. Nielsen A. M. Molenbroek, and J. R. Rostrup-Nielsen, " Steam Reforming and Graphite Formation on Ni Catalysts", **Journal of Catalysis**, 2002, 209, 365-384.

²⁵ E. Perry Murray, T. Tsai, and S.A. Barnett, "A direct-methane fuel cell with a ceria-based anode," **Nature**, 1999, **400**:651-659.

²⁶ S. Park, J.M. Vohs, and R.J. Gorte, "Direct oxidation of hydrocarbons in a solid-oxide fuel cell," **Nature**, 2000, **404**: 265-266.

²⁷ Jiang SP, Chan HC, “A review of anode materials development in solid oxide fuel cell”, **Journal of Material Science**, 2004, **39**: p. 4405-4439

²⁸ B. de Boer, PhD Thesis, University of Twente, Twente, The Netherlands (1998)

²⁹ Stig Helveg, Carlos Lopez-Cartes, Jens Sehested, Poul L. Hansen, Bjerne S. Clausen, Jens R. Rostrup-Nielsen, Frank Abild-Pedersen, Jens K. Nørskov, “*Atomic-scale imaging of carbon nanofibre growth*”, *Nature*, 2004, **427**, 426

³⁰ S. Helveg, C.L.-Cartes, J. Sehested, P.L. Hansen, B.S. Clausen, J. R. Rostrup-Nielsen, F.A. Pedersen, J.K. Nørskov, “Atomic-scale imaging of carbon nanofibre growth”, **Nature**, 2004, **427**: 426-429.